View metadata, citation and similar papers at core.ac.uk

brought to you by CORE

provided by Catalogo dei prodotti della ricerca

Developmental Cell, Vol. 4, 799–812, June, 2003, Copyright ©2003 by Cell Press

Control of Meiotic and Mitotic Progression by the F Box Protein β-Trcp1 In Vivo

Daniele Guardavaccaro,[1] Yasusei Kudo,[1,5] Jérôme Boulaire,[1] Marco Barchi,[2] Luca Busino,[1,3] Maddalena Donzelli,[3] Florence Margottin-Goguet,[4] Peter K. Jackson,[4] Lili Yamasaki,[2] and Michele Pagano[1,*]

[1]Department of Pathology and
New York University Cancer Institute
New York University School of Medicine
New York, New York 10016

[2]Biological Sciences
Columbia University
New York, New York 10027

[3]European Institute of Oncology
20141 Milan
Italy

[4]Department of Pathology
Stanford University School of Medicine
Stanford, California 94305

Summary

SCF ubiquitin ligases, composed of three major subunits, *S*kp1, *C*ul1, and one of many *F box p*roteins (Fbps), control the proteolysis of important cellular regulators. We have inactivated the gene encoding the Fbp β-Trcp1 in mice. β-Trcp1$^{-/-}$ males show reduced fertility correlating with an accumulation of methaphase I spermatocytes. β-Trcp1$^{-/-}$ MEFs display a lengthened mitosis, centrosome overduplication, multipolar metaphase spindles, and misaligned chromosomes. Furthermore, cyclin A, cyclin B, and Emi1, an inhibitor of the anaphase promoting complex, are stabilized in mitotic β-Trcp1$^{-/-}$ MEFs. Indeed, we demonstrate that Emi1 is a bona fide substrate of β-Trcp1. In contrast, stabilization of β-catenin and IκBα, two previously reported β-Trcp1 substrates, does not occur in the absence of β-Trcp1 and instead requires the additional silencing of β-Trcp2 by siRNA. Thus, β-Trcp1 regulates the timely order of meiotic and mitotic events.

Introduction

*F box p*roteins (Fbps) are characterized by an approximately 40 amino acid motif called the F box as it was first identified in cyclin F (Bai et al., 1996). Fbps play a crucial role in the ubiquitin-mediated degradation of cellular regulatory proteins, being subunits of ubiquitin ligases named SCFs because they are formed by the basic components *S*kp1, *C*ul1, Roc1/Rbx1, and one of many *F*bps (reviewed by Kipreos and Pagano, 2000). Because the substrate specificity of SCF ligases is dictated by different Fbps that act as substrate-targeting subunits, large families of Fbps are present in all eukaryotes to ensure high specificity.

Mammalian β-Trcp1 (β-*t*ransducin *r*epeat *c*ontaining *p*rotein, also called Fbw1a) has been reported to be involved in the degradation of IκB family members in response to NFκB activating stimuli (Yaron et al., 1998; Hatakeyama et al., 1999; Hattori et al., 1999; Kroll et al., 1999; Spencer et al., 1999; Shirane et al., 1999; Winston et al., 1999; Wu and Ghosh, 1999). In addition, mammalian β-Trcp1 controls β-catenin stability (Hart et al., 1999; Hatakeyama et al., 1999; Kitagawa et al., 1999; Latres et al., 1999). All well-characterized substrates of β-Trcp1 have a conserved destruction motif, DSGxxS, and are recognized by this Fbp only upon phosphorylation of the two serine residues present in this motif. A further level of complexity is added by the presence of a β-Trcp1 paralogous gene product, called β-Trcp2. β-Trcp1 and β-Trcp2 are ubiquitously expressed in both human and mouse tissues (Cenciarelli et al., 1999; Koike et al., 2000; Maruyama et al., 2001). In addition, β-Trcp2 has biochemical properties similar to β-Trcp1 in its ability to sustain the ubiquitinylation of both β-catenin and IκB family members in vitro and to control their degradation in overexpression experiments performed in mammalian cultured cells (Fuchs et al., 1999; Tan et al., 1999; Suzuki et al., 1999). Thus, it is not clear whether these two Fbps have overlapping functions in vivo or whether each of them recognizes specific substrates. To investigate the role of β-Trcp1 in normal growth and development and to determine the substrate selectivity of β-Trcp1 in vivo, we have inactivated the gene encoding this protein in mice by homologous recombination. The results of these studies are herein presented.

Results

Generation of β-Trcp1$^{-/-}$ Mice

A targeting construct was designed to delete codons 154–212 of the gene encoding mouse β-Trcp1, thus removing all but four amino acids of the F box plus an additional 22 amino acid region downstream of the F box (Figure 1A). Chimeric mice were generated that gave germline transmission of the mutant allele. Intercrossing of heterozygous mice yielded β-Trcp1$^{-/-}$ animals, as determined by Southern blot analysis (Figure 1B) and genomic PCR (Figure 1C). Northern blot (Figure 1D) and Western blot (Figure 1E) analyses revealed that insertion of the *neo*^{R} gene in the opposite transcriptional orientation prevented expression of β-Trcp1 in mouse embryonic fibroblasts (MEFs) and all tissues analyzed (not shown). β-Trcp1 deficiency did not affect the viability of β-Trcp1$^{-/-}$ animals, as shown by the fact that intermating of β-Trcp1$^{+/-}$ mice yielded viable β-Trcp1$^{+/+}$, β-Trcp1$^{+/-}$, and β-Trcp1$^{-/-}$ mice at approximately the expected Mendelian ratio (27.12%, 49.62%, and 23.25%, respectively; n = 800).

No obvious difference between the overall health status of β-Trcp1-deficient mice and wild-type mice was evident during more than 2 years of observation. Similarly, autopsy did not show gross tissue abnormalities in β-Trcp1$^{-/-}$ mice. The only exceptions that we observed were one invasive adenocarcinoma of the intestine observed in a 10-month-old β-Trcp1$^{-/-}$ mouse and the

*Correspondence: michele.pagano@med.nyu.edu
[5]This author is on sabbatical leave from Hiroshima University.

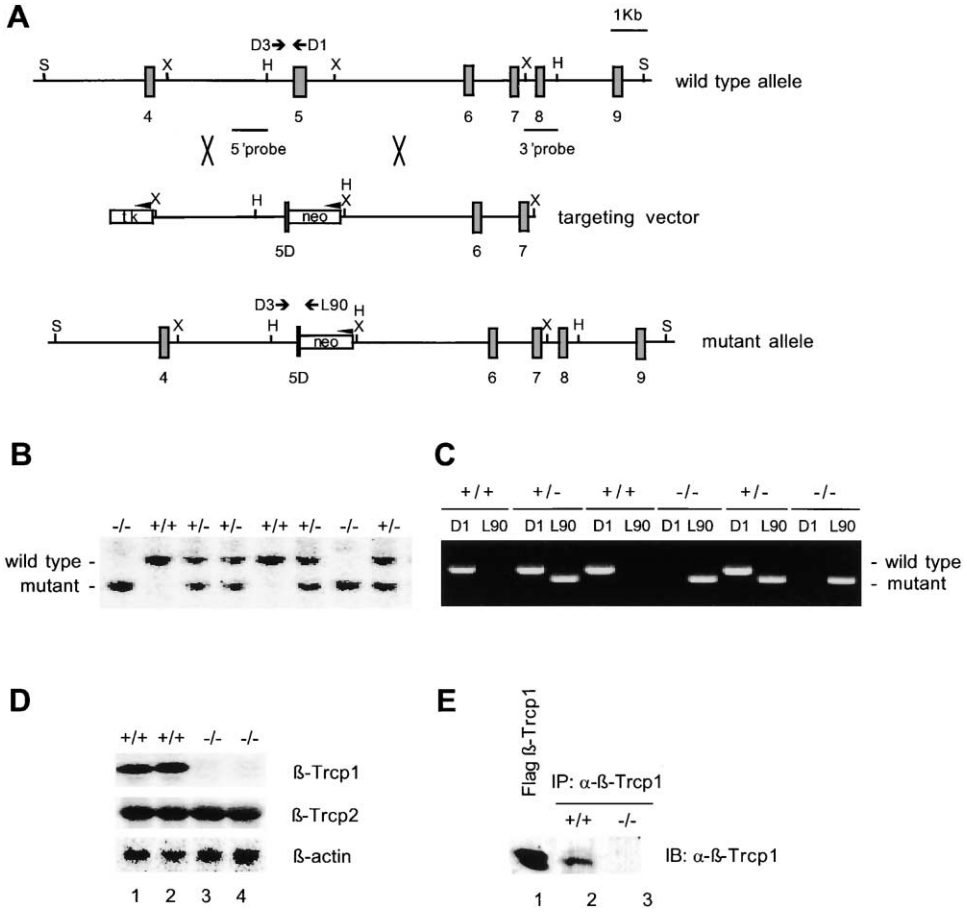

Figure 1. Generation of β-Trcp1$^{-/-}$ Mice

(A) Genomic organization of the wild-type gene encoding mouse β-Trcp1 is shown (top) with the position of coding exons 4–9 indicated. To generate the targeting vector (middle), the *neo*^{R} gene was inserted in an antisense orientation to replace codons 154–212 corresponding to all but four amino acids of the F box of β-Trcp1 plus an additional 22 amino acid region downstream of the F box. Homologous recombination between the wild-type allele and the targeting vector produced the mutant allele (bottom).

(B) Southern blot analysis of wild-type, heterozygous, and homozygous mutant mice. After HindIII digestion, hybridization with a 3′ external probe detects an 8.2 Kbp wild-type allele and a 6.0 Kbp mutant allele.

(C) A genomic PCR analysis was performed to genotype all progeny. Separate PCR reactions with either the unique exon primer (D1) or the unique neo primer (L90) and a common intron primer (D3) (see PCR primer positions in [A]) were used to detect the wild-type or the mutant allele, respectively.

(D) Expression of β-Trcp1 and β-Trcp2 transcripts. Total RNAs were prepared from different batches of MEFs from β-Trcp1$^{+/+}$ (lanes 1 and 2) and β-Trcp1$^{-/-}$ (lane 3 and 4) mice and processed for Northern blotting using full-length mouse β-Trcp1 (upper panel), β-Trcp2 (middle panel), or β-actin cDNA (lower panel).

(E) Expression of β-Trcp1 protein. Lane 1: recombinant Flag-tagged β-Trcp1 used as a marker. Extracts from β-Trcp1$^{+/+}$ (lane 2) and β-Trcp1$^{-/-}$ MEFs (lane 3) were subjected to immunoprecipitation (IP) with an antibody to β-Trcp1 followed by immunoblotting analysis (IB) with the same antibody.

premature death of two β-Trcp1$^{-/-}$ mice from thymic lymphomas at 6.5 and 19 months of age.

Reduced Fertility and Accumulation of Metaphase I Spermatocytes in β-Trcp1-Deficient Males

Although copulatory behavior was normal and vaginal plugs were produced, β-Trcp1$^{-/-}$ males have a fertility defect. In breeding experiments, 50% of the tested β-Trcp1$^{-/-}$ males never produced progeny with young fertile wild-type females (Table 1). In addition, the remaining 50% showed reduced fertility, as judged by the number of litters generated and the mean litter size (Table 1). Histological evaluation of the lumen of epididymes from adult β-Trcp1$^{-/-}$ males (Figures 2B and 2D) showed a strong reduction of mature spermatozoa and the presence of abnormal cells and cellular debris not found in wild-type mice (Figures 2A and 2C; n = 11, β-Trcp1$^{-/-}$ males and n = 9, wild-type males). Figures 2E–2I show histological sections of testes from control and knockout adult mice. Seminiferous tubules at stage VII showed a number of irregularities, including the formation of vacuoles and a smaller number of round spermatids arranged in irregular patterns (Figure 2F). In addition, multinucleated cells (arrows in Figure 2F), which appear to be abnormal round spermatids, were present. Frequently, these multinucleated cells were very large in size and contained nuclei of different sizes within the same single cell (Figure 2I). β-Trcp1$^{-/-}$ seminiferous

Table 1. β-Trcp1$^{-/-}$ Male Mice Have Reduced Fertility

Genotype	Fraction Fertile (Fertile/Total)	Litters/Fertile Pair (n)	Mean Litter Size (n)
β-Trcp1$^{+/+}$	4/4	6.5	7.8
β-Trcp1$^{+/-}$	10/10	6.4	7.5
β-Trcp1$^{-/-}$	5/10	3.2	2.1

Males (8–12 weeks of age) of the three different genotypes were tested for fertility for a period of approximately 4 months with both virgin and experienced young wild-type females. Copulatory behavior was judged to be normal and vaginal plugs were regularly found. Fifty percent of β-Trcp1$^{-/-}$ mice were sterile and the remaining 50% had reduced fertility as judged by the number of litters generated ($p = 0.009$) and the mean litter size ($p = 0.001$).

tubules at stage XII showed unusual chromatin figures and the absence of elongated spermatids facing the lumen (compare Figures 2G and 2H). We also noticed that compared to wild-type littermate controls, a larger number of metaphase I spermatocytes (characterized by the dark metaphase plate) per tubule at stages XII is present in β-Trcp1$^{-/-}$ mice (13.6 ± 1.7 in β-Trcp1$^{-/-}$ and 8.0 ± 0.3 in β-Trcp1$^{+/+}$; $n = 4$ for each group; $p = 0.005$; Figure 2H). Moreover, a fraction of spermatocytes displayed spindle abnormalities and misaligned chromosomes (not shown). The histopathologic defects in different β-Trcp1$^{-/-}$ mice paralleled their fertility impairment, as sterile animals showed more severe abnormalities than those observed in mice with reduced fertility.

Altogether, our data indicate that a prolonged and abnormal meiosis in spermatocytes may be responsible for the reduction of postmeiotic spermatids in testes and mature spermatozoa in epididymes with the consequent reduced fertility in β-Trcp1-deficient males. Thus, these results reveal a role for β-Trcp1 in the control of meiosis.

Mitotic Defects and Centrosomal Overduplication in β-Trcp1$^{-/-}$ MEFs

To determine whether the meiotic defects observed in germ cells corresponds to a mitotic defect in somatic cells, we used MEFs, where cell cycle alterations can be studied in greater detail than in vivo. We prepared MEFs from β-Trcp1$^{+/+}$ and β-Trcp1$^{-/-}$ embryos and examined their cell cycle properties in culture. The cell cycle profiles of asynchronous early-passage β-Trcp1$^{-/-}$ and β-Trcp1$^{+/+}$ MEF cultures were very similar, as revealed by flow cytometry analysis (Figure 3A). We then investigated the progression from G1 into S phase. β-Trcp1$^{-/-}$ and β-Trcp1$^{+/+}$ MEFs were arrested in G0/G1 by serum deprivation and then reactivated with serum. Following reentry into the cell cycle, the kinetics of S phase entry were similar in the two genotypes (Figures 3A and 3B). In contrast, when we analyzed the progression through mitosis, we observed significant differences. Cells were arrested in prometaphase using nocodazole treatment followed by mitotic shake-off. At various times after replating in fresh medium, cells were collected and specific mitotic forms were analyzed by immunofluorescence (Figures 3C and 3D). Forty-five minutes after replating, 51.1 ± 5.3% of β-Trcp1$^{-/-}$ MEFs were either in prometaphase, metaphase, or anaphase, while only 20.1 ± 6.2% of wild-type cells were still at these mitotic stages. By 75 minutes, the differences were less dramatic, with 85.1% of wild-type cells having exited mitosis and entered the next G1, whereas 26.0% of the β-Trcp1$^{-/-}$ cells were unable to do so and remained in mitosis.

We also analyzed centrosomes and mitotic spindles in asynchronous populations of early-passage MEFs. Most cells from β-Trcp1$^{+/+}$ and β-Trcp1$^{+/-}$ mice contained one or two centrosomes juxtaposed to the nucleus. In contrast, a significant fraction of β-Trcp1$^{-/-}$ MEFs contained more than two centrosomes (3–12 per cell; Figure 4A). Quantitative analysis revealed that abnormal amplification of the centrosomes was present in 21.5 ± 1.9% of β-Trcp1$^{-/-}$ MEFs compared with a value of 3.2 ± 2.8% for β-Trcp1$^{+/+}$ MEFs (Figure 4B). As shown in Figure 4A, centrosome splitting occurs regularly in β-Trcp1$^{-/-}$ MEFs, as the supernumerary centrosomes appeared well separated from each other. In addition, 11.6% of the mitotic β-Trcp1$^{-/-}$ MEFs showed multipolar spindles (Figure 4C), indicating that at least a fraction of the supernumerary centrosomes is mature as spindles organizers. In turn, the abnormalities in spindle structures are likely to be the cause of the misalignment of chromosomes from the metaphase equator observed by staining condensed chromosomes with an anti-phospho-specific antibody to Histone H3 (Figure 4C).

A prolonged S phase or mitosis can result in centrosome overduplication. β-Trcp1$^{-/-}$ MEFs show a delay in progressing through mitosis but not through the G1-S transition. Thus, the centrosomal overduplication of mutant cells could be attributable to the mitotic defect. Significantly, the mitotic defects of β-Trcp1$^{-/-}$ MEFs are consistent with the meiotic phenotype observed in germ cells.

Stabilization of Mitotic Regulators in β-Trcp1$^{-/-}$ MEFs and Testes

Because β-Trcp1-deficient MEFs displayed delayed mitotic progression, we analyzed the expression of cell cycle regulatory proteins. In agreement with the data concerning DNA replication (Figures 3A and 3B), following reentry into the cell cycle, levels of cyclin A and cyclin B gradually increased with similar kinetics in wild-type and mutant cells (Figure 5A). We then analyzed the levels of these cell cycle regulators during the M-to-G1 transition. Prometaphase cells were allowed to synchronously progress through mitosis and enter into the next G1 phase. Significant differences between the two genotypes were consistently observed in multiple experiments using different batches of early-passage MEFs obtained from β-Trcp1$^{-/-}$ and littermate control mice (a representative example is shown in Figure 5B). As expected (Girard et al., 1995), cyclin A and cyclin B were present in

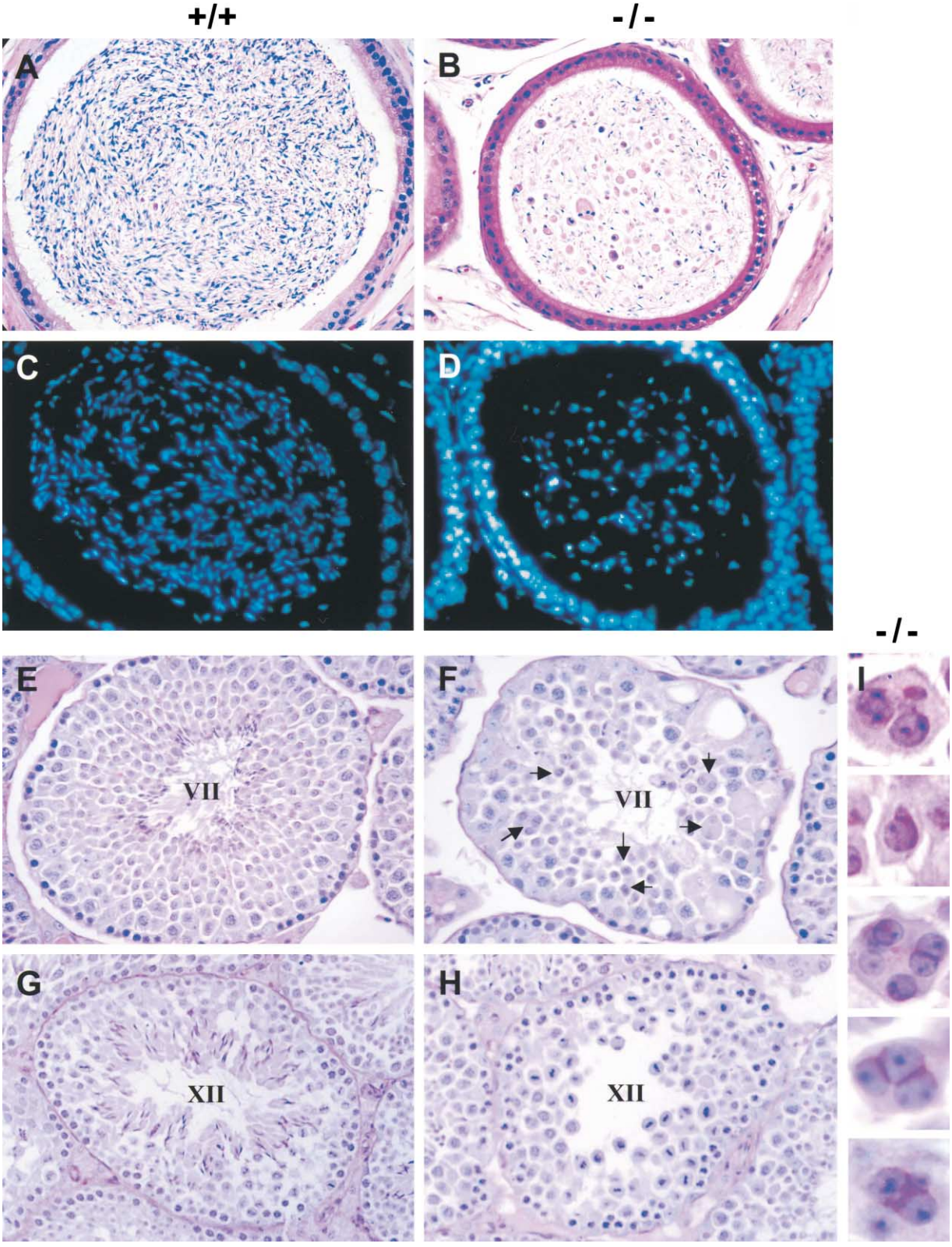

Figure 2. Defective Spermatogenesis and Accumulation of Metaphase I Spermatocytes in β-Trcp1$^{-/-}$ Mice

(A–D) Histology of epididymis. The histological sections were stained with H&E (A and B) and DAPI (C and D). The panels to the left (A and C) show the epididymis histology of wild-type mice; the panels to the right (B and D), that of β–Trcp1$^{-/-}$ animals.

(E–I) Testicular histology. The panels to the left (E and G) show the testicular histology of wild-type mice; the panels to the right (F, H, and I), that of β-Trcp1-deficient animals. Top panels show seminiferous tubules at stage VII (E and F); bottom panels show seminiferous tubules at stage XII (G and H). Arrows in (F) point to multinucleated cells (some of which are magnified in [I]).

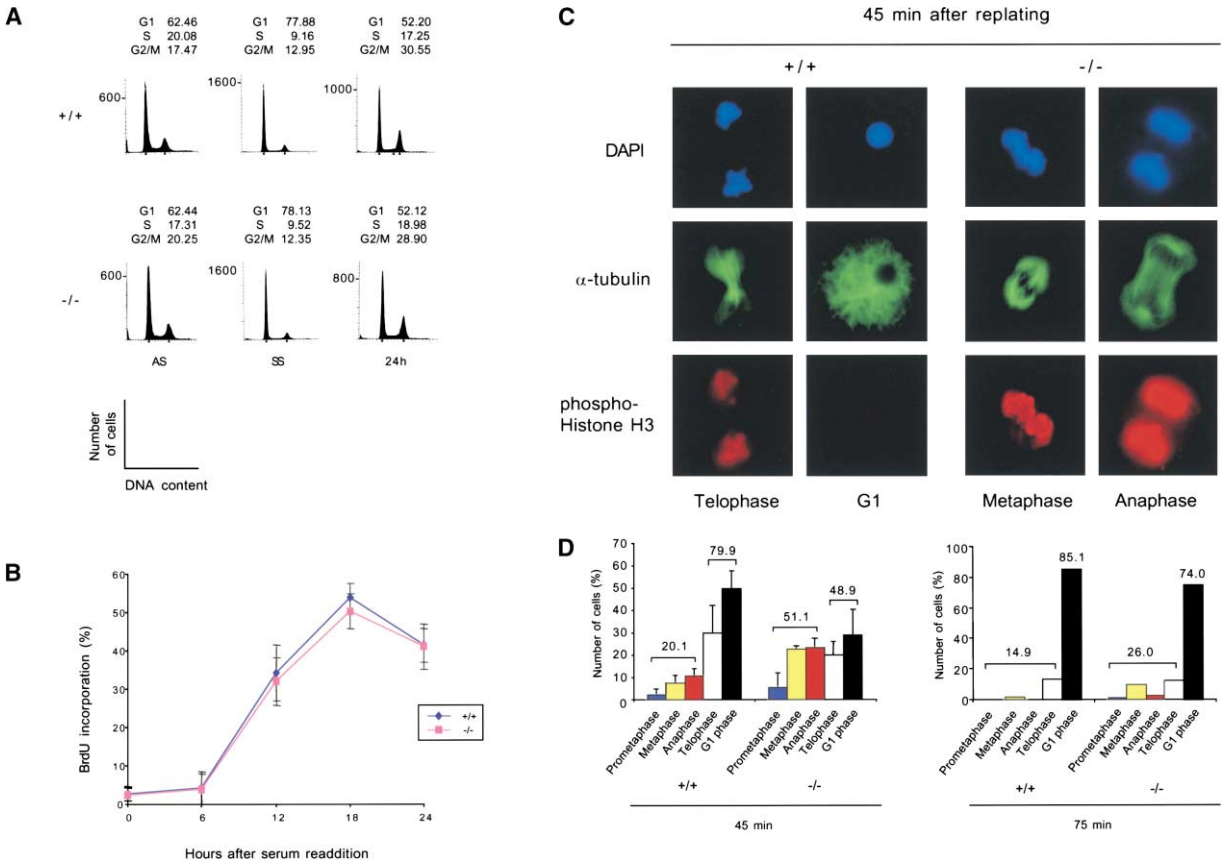

Figure 3. Mitotic Phenotype in β-Trcp1$^{-/-}$ MEFs

(A) Flow cytometry profiles of β-Trcp1$^{+/+}$ (top) and β-Trcp1$^{-/-}$ MEFs (bottom). Asynchronous populations (AS) were serum starved for 72 hr (SS), trypsinized, and then reactivated to reenter the cell cycle with 20% serum for 24 hr.

(B) Time course of DNA synthesis after reactivation with serum. DNA synthesis was monitored by adding BrdU in the last 2 hr of culture followed by immunostaining at the time points indicated in the figure.

(C and D) β-Trcp1$^{-/-}$ MEFs show a prolonged mitosis.

(C) MEFs were stained 45 min after release from prometaphase with DAPI (to visualize DNA), an anti-α-tubulin antibody (to visualize microtubules and identify mitotic forms), and an anti-phospho-specific antibody to Histone H3 (to visualize condensed chromosomes characteristic of mitotic cells).

(D) Specific mitotic forms were quantified at different times after release from prometaphase. The results shown on the left are the mean percentage obtained from four independent experiments using different batches of early-passage MEFs obtained from β-Trcp1$^{-/-}$ and littermate control mice.

both wild-type and β-Trcp1$^{-/-}$ prometaphase cells, but disappeared with significantly different kinetics. By 45 min, most cyclin A was degraded in β-Trcp1$^{+/+}$ MEFs but approximately 50% was still present in β-Trcp1-deficient cells. Likewise, cyclin B degradation was delayed in β-Trcp1$^{-/-}$ MEFs.

Because β-Trcp1-deficient cells progress slowly through mitosis and degrade both cyclin A and cyclin B with delayed kinetics, we reasoned that the APC/C (*a*naphase *p*romoting *c*omplex/*c*yclosome) might be inhibited in these cells. A well-established negative regulator of APC/C is Emi1 (*e*arly *m*itotic *i*nhibitor 1), which is upregulated during S and G2 and degraded early in mitosis to allow for the activation of APC/C (Hsu et al., 2002). We therefore analyzed the levels of Emi1 during cell cycle progression. Whereas Emi1 expression during the G1-to-S transition was similar in wild-type and mutant MEFs (Figure 5A), Emi1 was present in prometaphase β-Trcp1-deficient MEFs but not in prometaphase β-Trcp1$^{+/+}$ cells (Figure 5B, compare lanes 1 and 5). When prometaphase β-Trcp1$^{-/-}$ MEFs progressed through mitosis, Emi1 levels slowly decreased (Figure 5B, lanes 6–8). At later time points, when most cells had entered G1, Emi1 was almost totally degraded (Figure 5B, lane 10). We also looked at the progression through mitosis using a different synchronization method. Cells were arrested in early S phase by first culturing in medium containing low serum and then releasing them into complete medium containing aphidicolin. MEFs were harvested at different times after release from the S phase block and analyzed by immunoblotting for the levels of mitotic regulatory proteins (Figure 5C). Entry into mitosis was examined with an anti-phospho-specific antibody to Histone H3 used in immunoblotting (Figure 5C) and immunofluorescence (not shown). Although the majority of MEFs from both genotypes reached mitosis by 9 hr after aphidicolin release, a lengthened progression through mitosis and a delayed

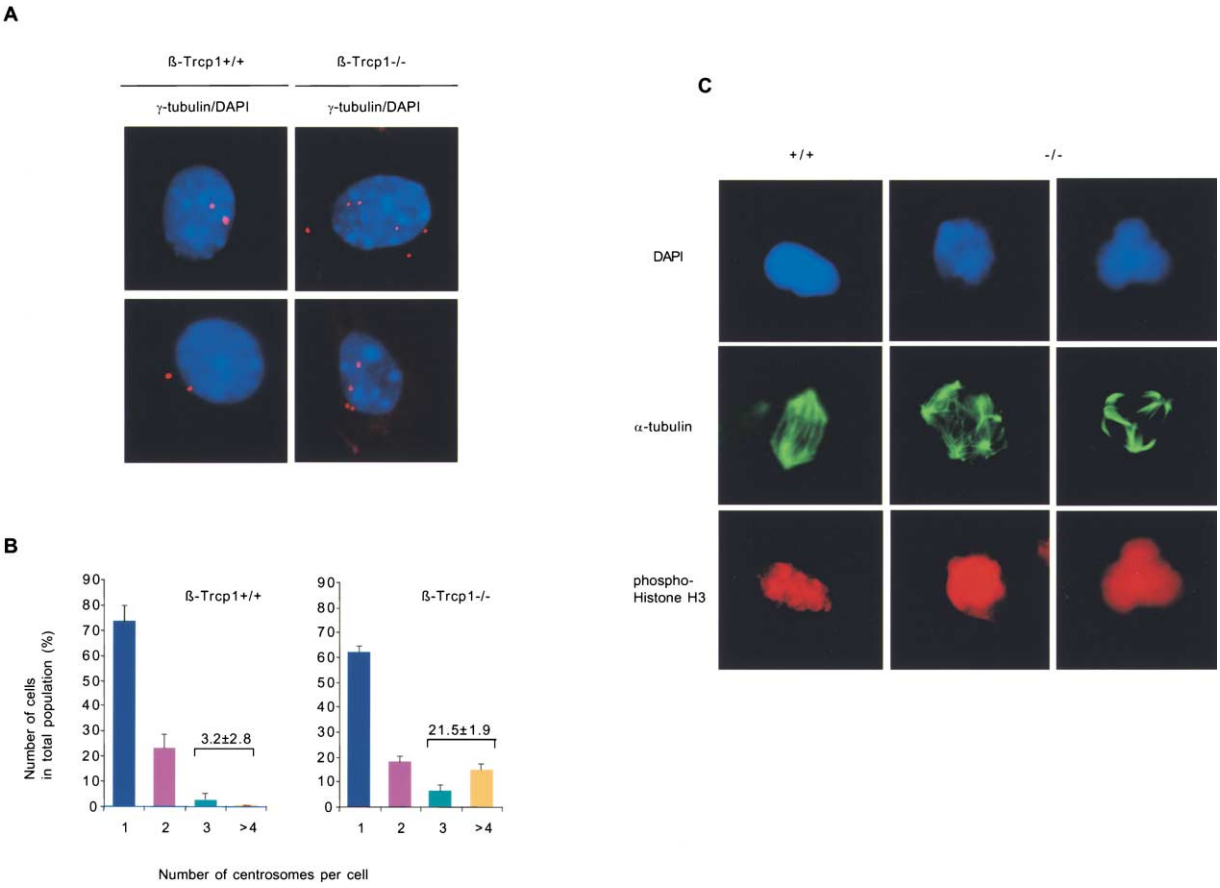

Figure 4. β-Trcp1$^{-/-}$ MEFs Display Centrosome Overduplication, Multipolar Spindles, and Misaligned Chromosomes

(A and B) Overduplication of centrosomes in β-Trcp1$^{-/-}$ MEFs.

(A) MEFs from β-Trcp1$^{+/+}$ (two panels on the left) and β-Trcp1$^{-/-}$ (two panels on the right) mice were stained with anti-γ-tubulin antibody (red) to stain the centrosomes and with DAPI (blue) to stain DNA.

(B) Quantitative analysis of centrosome number. Data are expressed as the percentage of cells that contained the indicated number of centrosomes.

(C) Multipolar spindles and misaligned chromosomes in β-Trcp1$^{-/-}$ cells. MEFs were stained with DAPI (to visualize DNA), an anti-α-tubulin antibody (to visualize mitotic spindles), and an anti-phospho-specific antibody to Histone H3 (to visualize condensed chromosomes).

kinetics of degradation for Emi1 and cyclin A were observed in β-Trcp1$^{-/-}$ MEFs. Thus, in wild-type MEFs, Emi1 has the expected timing of expression and degradation (Hsu et al., 2002), whereas in β-Trcp1-deficient MEFs it behaves aberrantly, accumulating in prometaphase. Importantly, this accumulation correlated with a stabilization of the protein as shown by measuring its half-life by two different methods. First, prometaphase cells were incubated with cycloheximide to inhibit protein synthesis, and then the rate of Emi1 degradation was followed by immunoblotting (Figure 5D, second panel from the top). We also estimated Emi1 degradation by a pulse-chase procedure, but due to the limited size of early-passage MEF cultures, we could not use a pure population of cells in prometaphase. We therefore enriched the G2-M population by incubating the MEF culture with nocodazole prior to the pulse-chase with ^{35}S-labeled amino acids (Figure 5D, bottom panel). The half-life of Emi1 measured in wild-type cells is consistent with a mixed population consisting of mitotic cells, in which Emi1 has a short half-life, and G2 cells, in which Emi1 is stable. In fact, approximately 50% of Emi1 is degraded in 45 min but then the remaining fraction is stable for up to 75 min. In contrast, Emi1 is completely stable in β-Trcp1$^{-/-}$ MEFs.

Finally, we analyzed levels of Emi1, cyclin A, and two previously reported β-Trcp1 substrates (IκBα and β-catenin) in 16 different mouse organs from wild-type and β-Trcp1-deficient mice (representative examples are shown in Figure 5E). We observed an accumulation of Emi1 and cyclin A in testes of β-Trcp1$^{-/-}$ mice but not in other organs. The extent of this accumulation is likely to be underestimated, as the extract from testes also included a majority of nonmetaphase cells in which, based on the results in MEFs, β-Trcp1 deficiency is not predicted to affect Emi1 levels.

Emi1 Is a Bona Fide Substrate of β-Trcp1

After observing a stabilization of Emi1 in β-Trcp1$^{-/-}$ MEFs, we noticed that this protein contains a DSGxxS β-Trcp1 binding domain that is conserved among species (Figure 6A), suggesting that Emi1 might be a direct substrate of β-Trcp1. To test this possibility, we transfected MEFs with Myc-tagged wild-type Emi1 or an Emi1

mutant in which both serine residues of the DSGxxS motif have been mutated to alanine [Emi1(S145A/S149A) mutant]. We then synchronized cells in prometaphase, measured Emi1 half-life by the addition of cycloheximide, and found that wild-type Emi1 was stabilized in β-Trcp1$^{-/-}$ cells (Figure 6B, second panel from the top). In contrast, Emi1(S145A/S149A) mutant was stable in MEFs from both genotypes (Figure 6B, bottom panel). To test whether a difference in Emi1 degradation corresponds to a difference in its ubiquitinylation, we developed a cell-free assay for Emi1 ubiquitinylation using extracts from prometaphase MEFs. Using this assay, we found that Emi1-ubiquitin ligation activity is higher in an extract from wild-type prometaphase MEFs than from β-Trcp1-deficient prometaphase MEFs (Figure 6C, lanes 1–8). Emi1(S145A/S149A) mutant was not ubiquitinylated by either extract (not shown). Importantly, the addition of a recombinant purified SCF$^{\beta\text{-Trcp1}}$ complex to a prometaphase extract of β-Trcp1$^{-/-}$ cells strongly rescues its ability to ubiquitinylate Emi1 (Figure 6C, lanes 9–12), whereas recombinant purified SCF^{Skp2} complex had no effect (not shown). Thus, the in vitro data are in agreement with the in vivo results and indicate that the defect in Emi1 degradation observed in β-Trcp1$^{-/-}$ MEFs is due to its lack of β-Trcp1-mediated ubiquitinylation.

Because SCF substrates interact with the Fbps that target them for ubiquitinylation, we asked whether β-Trcp1 and Emi1 physically interact in cultured cells. Mammalian expression plasmids carrying either Flag-tagged β-Trcp1, Flag-tagged Fbw4, or Flag-tagged Fbw5 (two Fbps that, like β-Trcp1, contain WD-40 domains) were transfected in HeLa cells. Endogenous Emi1 was coimmunoprecipitated only with Flag-tagged β-Trcp1 (Figure 6D, lanes 1–4). To test whether this interaction is mediated by the DSGxxS motif of Emi1, we expressed Flag-tagged β-Trcp1 together with Myc-tagged Emi1 (either wild-type or mutant). Emi1 but not Emi1(S145A/149A) mutant was detected in anti-Flag immunoprecipitates (Figure 6D, lanes 5–7), confirming the importance of Ser145 and Ser149 in mediating the association between Emi1 and β-Trcp1.

Taken together, these results demonstrate that Emi1 is a bona fide substrate of β-Trcp1, which likely accounts for the stabilization of Emi1 observed in prometaphase β-Trcp1$^{-/-}$ MEFs.

Stabilization of IκBα and β-Catenin Requires the Silencing of Both β-Trcp1 and β-Trcp2

A large body of literature reports that IκBα and β-catenin are two major putative substrates of β-Trcp1. We therefore examined whether the degradation of IκBα was affected by the absence of β-Trcp1. NFκB activity was stimulated in wild-type and β-Trcp1-deficient MEFs with *t*umor *n*ecrosis *f*actor-α (TNFα; Figure 7A), IL-1 (Figure 7B), *l*ipo*p*oly*s*accharide (LPS; Figure 7C), or a variety of other stimuli or stresses (i.e., PMA, sorbitol, tunicamycin, H_2O_2, and UV; data not shown). We also stimulated thymocytes with TNFα (Figure 7D) and macrophages with LPS (Figure 7E). At different times after stimulation, cells were collected and lysed, and cell extracts were used for either immunoblotting or to measure NFκB DNA binding activity by electrophoretic mobility shift assay. We consistently observed normal induction of IκBα degradation and resynthesis in β-Trcp1$^{-/-}$ cells with any stimulus and in all cell types tested. NFκB DNA binding activity was either identical in the two genotypes or occasionally reduced in β-Trcp1$^{-/-}$ cells (compare lanes 3 and 4 to lanes 7 and 8 in Figures 7D and 7E).

Basal levels of β-catenin are identical in β-Trcp1$^{+/+}$ and β-Trcp1$^{-/-}$ MEFs (Figure 7F, lanes 1 and 2), as well as in a number of tissues examined (Figure 5E). We tested whether β-catenin degradation was impaired after release from a Wnt3a-mediated β-catenin accumulation. After treatment with Wnt-3a for 2 hr, β-catenin increased substantially in both β-Trcp1$^{+/+}$ and β-Trcp1$^{-/-}$ cells (Figure 7F, lanes 3 and 7), and after Wnt3a withdrawal, levels of β-catenin were consistently and timely restored in MEFs from both genotypes (Figure 7F). Similarly, kinetics of β-catenin degradation were identical in MEFs from the two genotypes after a release from a treatment with lithium chloride used to stabilize β-catenin (not shown).

The result that the bulk of IκBα and β-catenin is degraded independently of β-Trcp1 prompted us to test whether β-Trcp2 was involved in regulating their stability. To this end, we used the small interfering RNA (siRNA) technique to reduce the expression of β-Trcp1 and β-Trcp2 in HeLa cells. When compared with HeLa cells transfected with a control double-stranded RNA (dsRNA) oligomer, cells transfected with two different dsRNA oligomers corresponding to β-Trcp1 showed no dramatic increase in the levels of β-catenin and, when stimulated with TNFα, they were still able to degrade IκBα (Figure 7G, lanes 4–6). This occurred despite the fact that these oligomers almost completely downregulated β-Trcp1 mRNA (Figure 7H, lane 2). Similar results were obtained when β-Trcp2 was silenced with a specific oligomer (Figure 7G, lanes 13–15; Figure 7H, lane 5). In contrast, when we used an oligomer efficiently targeting both β-Trcp1 and β-Trcp2 (Figure 7H, lane 3), we observed a dramatic accumulation of both β-catenin and IκBα (Figure 7G, lanes 7–9 and 16–18). In agreement with what was observed in β-Trcp1$^{-/-}$ MEFs, silencing of β-Trcp1 alone induced Emi1 stabilization in prometaphase HeLa cells (Figure 7I, lanes 5–8 and 10–12) and strongly delayed passage through mitosis (not shown). Interestingly, β-Trcp2 silencing also induced accumulation of Emi1 in prometaphase cells (Figure 7I, lanes 13–15), which is in agreement with the ability of β-Trcp2 to physically interact with Emi1 (not shown) similarly to β-Trcp1 (Figure 6D). Silencing of both β-Trcp1 and β-Trcp2 has a more profound effect on Emi1 stabilization as judged by measuring Emi1 half-life (Figure 7I, lanes 16–18).

Our data show that β-Trcp1 and β-Trcp2 are redundant in controlling the stability of β-catenin and IκBα, whereas either β-Trcp1 or β-Trcp2 is required to regulate Emi1 stability.

Discussion

A Role for β-Trcp1 in Meiosis and Mitosis

In this report, we show that β-Trcp1 loss of function in mice does not affect viability but induces an impairment of spermatogenesis and reduced fertility. This is likely

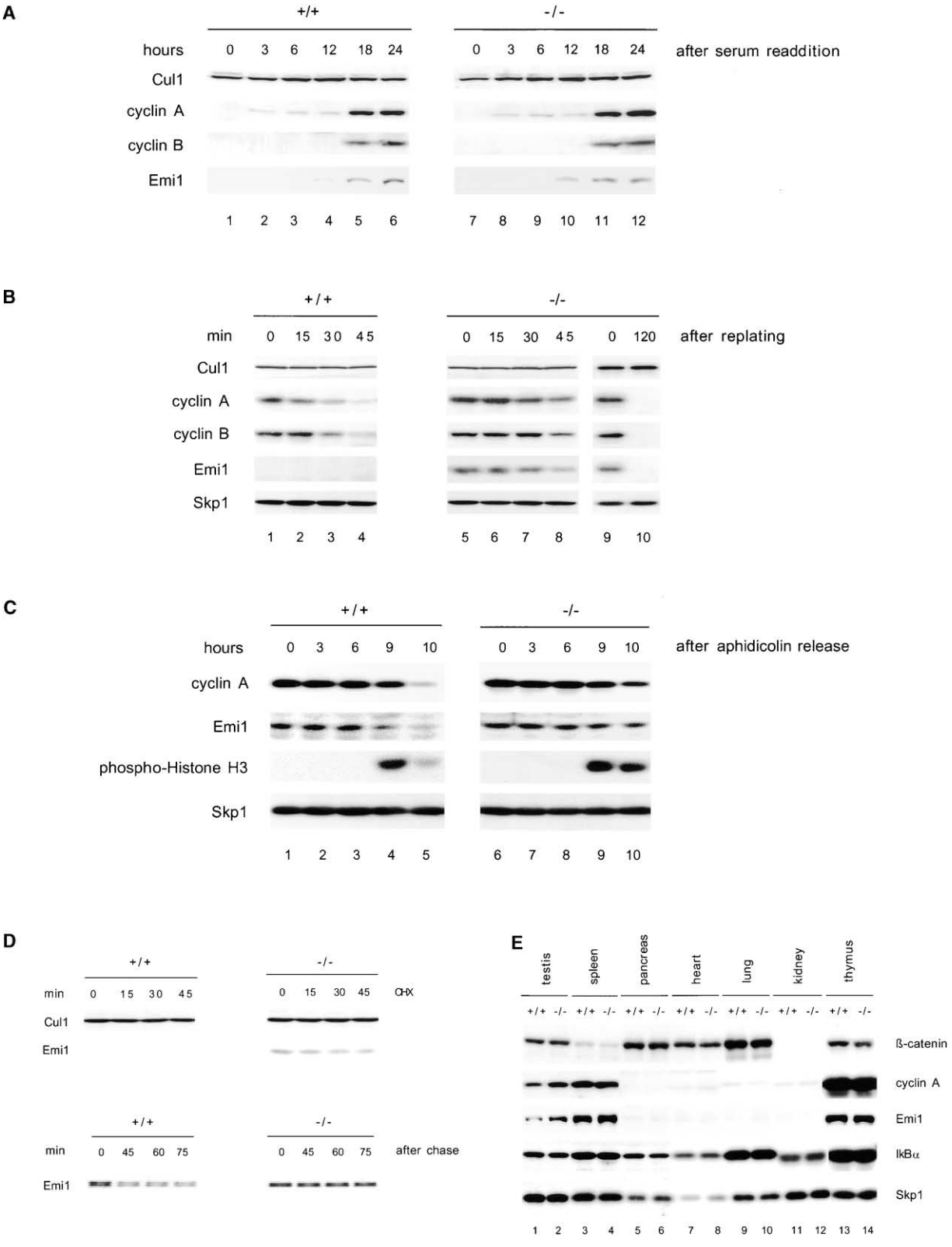

Figure 5. Stabilization of Mitotic Regulatory Proteins in β-Trcp1$^{-/-}$ MEFs and Testes

(A) Expression of cell cycle regulatory proteins in cells reentering the cell cycle from quiescence. β-Trcp1$^{+/+}$ MEFs (lanes 1–6) and β–Trcp1$^{-/-}$ MEFs (lanes 7–12) were synchronized in G0/G1 by serum deprivation (lanes 1 and 7; indicated as time 0), trypsinized, replated, and then reactivated with 20% serum. Cells were collected at the indicated times and protein extracts were analyzed by immunoblot with antibodies to the indicated proteins.

the result of the fact that a fraction of spermatocytes progresses slowly through meiosis (as shown by the accumulating metaphase I spermatocytes), whereas a different fraction appears to divide abnormally and eventually generate multinucleated spermatids. In turn, these defects result in a greatly reduced number of spermatids and spermatozoa.

A hypomorphic mutation in the gene encoding Slimb, the fly ortholog of β-Trcp1, causes the appearance of metaphase figures, condensed chromosomes, and polyploid figures in larval neuroblasts (Wojcik et al., 2000). This mitotic phenotype is reminiscent of the meiotic phenotype observed in mouse germ cells lacking β-Trcp1. To analyze mitotic progression in mouse somatic cells, we used MEFs and found that they have a lengthened mitosis. In addition, a fraction of β-Trcp1$^{-/-}$ MEFs displays centrosome overduplication associated with the presence of multipolar metaphase spindles and misaligned chromosomes. These mitotic defects are likely due to a stabilization of Emi1 specifically occurring in M phase. Emi1 is a regulator of both mitosis and meiosis (Hsu et al., 2002; Reimann et al., 2001; Grosskortenhaus and Sprenger, 2002; Reimann and Jackson, 2002) by virtue of inhibiting the ubiquitin ligase complex APC/C. This ubiquitin ligase controls the timely degradation of a variety of important mitotic regulatory proteins, a process that is necessary for the orderly progression through the cell division cycle (reviewed by Peters, 2002). During the G1 phase of the cell cycle, APC/C needs to be active to avoid any accumulation of mitotic cyclins. During S and G2, Emi1 accumulates to cooperate with cdks in inhibiting APC/C, thus allowing the accumulation of positive regulators of mitosis. Progression through and exit from M phase require the reactivation of APC/C. Our results strongly indicate that β-Trcp1 contributes to this reactivation by specifically mediating the degradation of Emi1 in early mitosis. In fact, in the absence of β-Trcp1, Emi1 is stabilized and mitotic cyclins accumulate, likely as the result of an Emi1-mediated inhibition of APC/C. Accordingly, overexpression of Emi1 in human cell lines (Hsu et al., 2002) and mouse cells (not shown) induces their accumulation in prometaphase and metaphase. In conclusion, the stabilization of Emi1 during M phase could explain why β-Trcp1$^{-/-}$ MEFs proceed more slowly through mitosis than wild-type cells. Similarly, the high levels of Emi1 found in testes of β-Trcp1-deficient mice are consistent with a stabilization of Emi1 in spermatocytes and could be the reason for the meiotic defects.

Several questions remain. Why is the most obvious phenotype in β-Trcp1-deficient mice reduced male fertility? Why is the penetrance of the phenotype found in β-Trcp1$^{-/-}$ testes incomplete? If, in addition to a role in meiosis, β-Trcp1 has a general role in somatic cells, why is the in vivo phenotype not more dramatic? One possible general answer to these questions is provided by the functional redundancy of the β-Trcp1 and β-Trcp2 gene products. Interestingly, although β-Trcp1 and β-Trcp2 transcripts are expressed to approximately the same extent in most organs, testis is the organ in which β-Trcp1 (both human and mouse) is expressed at the highest levels, whereas only low levels (as compared to those in other organs) of β-Trcp2 are expressed in this organ (Cenciarelli et al., 1999; Koike et al., 2000; Maruyama et al., 2001). Accordingly, among many organs examined, we observed an accumulation of Emi1 and cyclin A only in testes. There could be a further reason for which spermatocytes are particularly sensitive to β-Trcp1 deficiency. Spermatocytes undergo two rapid meiotic divisions without an intervening S phase to form haploid spermatids. Our data show that despite the delay in degradation, Emi1 disappears from β-Trcp1-deficient MEFs reentering G1, like for the action of a different ubiquitin ligase. Thus, two subsequent meiotic divisions, without the possibility to reset Emi1 levels as somatic cells do in G1, might translate into a more severe defect in spermatocytes than in somatic cells. Yet, despite Emi1 degradation being only decreased at M/G1 and not totally inhibited, in cultured MEFs it is possible to uncover a lengthened progression through mitosis that reveals an additional role for β-Trcp1 in somatic cells. In conclusion, the β-Trcp1 mouse knockout exposes an unexpected critical role for this Fbp in regulating the progression through both meiosis and mitosis.

Centrosomal Overduplication in the Absence of β-Trcp1

Cul1 and Skp1 play a key role in centriole splitting (reviewed by Hansen et al., 2002) as well as in later steps of the centrosome cycle, as shown by the fact that enforced expression of a Cul1 dominant-negative mutant induced multiple centrosome abnormalities, not only a failure of the centrioles to separate (Piva et al., 2002). Interestingly, a fraction of β-Trcp1$^{-/-}$ MEFs displays overduplication of centrosomes. Accordingly, a hypomorphic mutation in *Slimb* induces centrosome overduplication (Wojcik et al., 2000). The centrosome cycle is uncoupled from the cell division cycle because

(B) Expression of cell cycle regulators in cells released from a block in prometaphase. β-Trcp1$^{+/+}$ MEFs (lanes 1–4) and β-Trcp1$^{-/-}$ MEFs (lanes 5–10) were synchronized in prometaphase using nocodazole, and washed and replated in fresh medium. Cells were collected at the indicated times after release and protein extracts were analyzed by immunoblot with antibodies to the indicated proteins.

(C) Expression of cell cycle regulators in cells released from a block in early S phase. β-Trcp1$^{+/+}$ MEFs (lanes 1–5) and β-Trcp1$^{-/-}$ MEFs (lanes 6–10) were synchronized in early S phase using aphidicolin, washed, and then released from the block. Cells were collected at the indicated times after release and protein extracts were analyzed by immunoblot with antibodies to the indicated proteins.

(D) Stabilization of Emi1 in prometaphase β-Trcp1$^{-/-}$ MEFs. Prometaphase MEFs were plated in the presence of cycloheximide. At the indicated times, cells were collected and lysed, and extracts were subjected to immunoblotting with antibodies to Emi1 and Cul1 (top panels). In the experiment shown in the bottom panel, MEFs were incubated with nocodazole for 12 hr, labeled with [^{35}S]methionine and [^{35}S]cysteine for 45 min, and then chased with medium. At the indicated times, cells were collected and lysed, and extracts were subjected to immunoprecipitation with an anti-Emi1 antibody under denaturing conditions followed by SDS-PAGE and autoradiography.

(E) Emi1 and cyclin A accumulate in testes of β-trcp1$^{-/-}$ mice. Different organs were collected from three sterile β-Trcp1-deficient and three littermate wild-type mice. Extracts from testis (lanes 1 and 2), spleen (lanes 3 and 4), pancreas (lanes 5 and 6), heart (lanes 7 and 8), lung (lanes 9 and 10), kidney (lanes 11 and 12), and thymus (lanes 13 and 14) were immunoblotted with the antibodies to the indicated proteins.

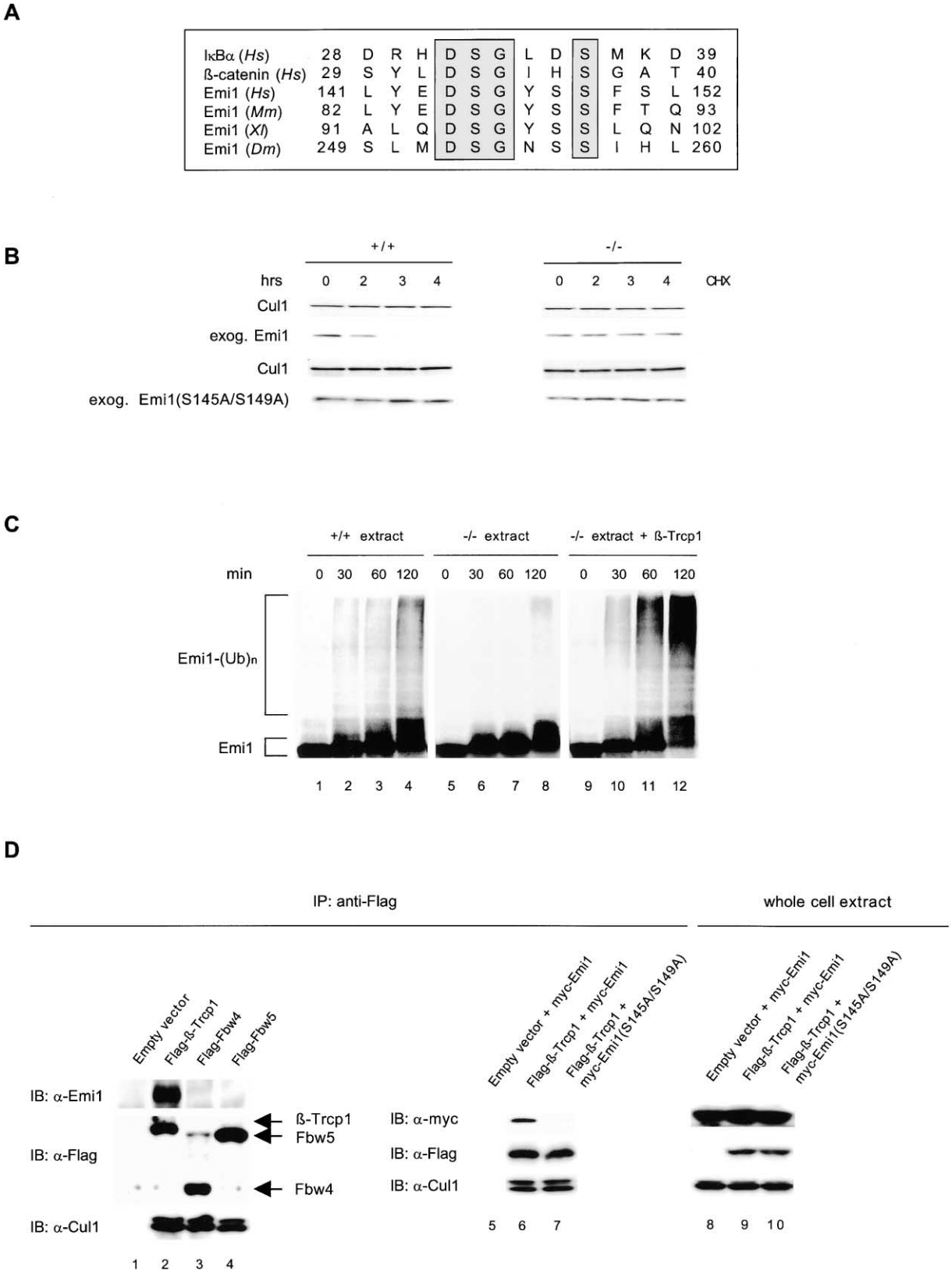

Figure 6. Emi1 Is a Bona Fide Substrate of β-Trcp1 In Vivo and In Vitro

(A) Alignment of the amino acid regions corresponding to the putative β-Trcp1 binding motif in Emi1 orthologs and in previously reported β-Trcp1 substrates.

(B) Wild-type Emi1 is only stable in β-Trcp1$^{-/-}$ MEFs, whereas Emi1(S145A/S149A) mutant is stable both in β-Trcp1$^{-/-}$ and β-Trcp1$^{+/+}$ MEFs.

centrosomal duplication can occur in cells arrested either at G1/S or in mitosis, hence generating multiple centrosomes per cell. β-Trcp1 deficiency might induce centrosomal overduplication by its ability to delay mitosis progression by increasing Emi1 levels and consequently inducing an inhibition of APC/C. In favor of this hypothesis is the fact that overexpression of Emi1 causes centrosomal overduplication and spindle abnormalities (our unpublished results) similar to what was observed in β-Trcp1-deficient MEFs. Furthermore, cyclin A, an established substrate of APC/C, accumulates in mitotic β-Trcp1-deficient cells. Because cyclin A is necessary for centrosomal division, we propose that the stabilization of cyclin A, associated with a lengthened mitosis, contributes to centrosomal overduplication. Of course, additional APC/C substrates, such as Aurora-A, Plk1, Cdc25a, and Nek2 might be stabilized as the result of APC/C inhibition by Emi1. In turn, the accumulation of these proteins could contribute to the amplification and separation of centrosomes in β-Trcp1$^{-/-}$ MEFs. In conclusion, β-Trcp1 cooperates with Cul1 and Skp1 in regulating the centrosome cycle.

β-Trcp1 Substrates

Herein we report that Emi1 is a bona fide substrate of β-Trcp1 both in vivo and in vitro. Importantly, the in vitro ubiquitinylation and the mitotic degradation of Emi1 are dependent on the availability of Ser145 and Ser149, which are present in a canonical β-Trcp1 binding site conserved in Emi1 orthologs. Indeed, these two serine residues are necessary for Emi1 to physically interact with β-Trcp1. Although β-Trcp1 is expressed throughout the cell cycle, its role in targeting Emi1 for degradation appears to be specific for mitosis because no accumulation of Emi1 is observed in β-Trcp1$^{-/-}$ cells progressing through G1 and into S phase (Figure 5A). Thus, it is possible that Ser145 and Ser149 are specifically phosphorylated in mitosis, allowing the recognition of Emi1 by β-Trcp1.

As detailed in the Introduction, a large number of studies has shown that β-Trcp1 is necessary for targeting IκBα and β-catenin for degradation. Yet, MEFs from β-Trcp1-deficient mice degrade both IκBα and β-catenin with kinetics similar to those observed in wild-type MEFs. Similarly, IκBα degradation is not inhibited in T cells or in macrophages. In addition, silencing of either β-Trcp1 or β-Trcp2 alone does not dramatically affect the stability of IκBα and β-catenin in HeLa cells, whereas downregulation of the levels of both β-Trcp1 and β-Trcp2 induces a dramatic accumulation of both substrates. Thus, we can conclude that β-Trcp1 and β-Trcp2 are redundant in controlling the stability of IκBα and β-catenin, whereas both β-Trcp1 and β-Trcp2 regulate Emi1 stability. IκBα is targeted for degradation only by homodimers of either β-Trcp1 or β-Trcp2 (Suzuki et al., 2000). The fact that silencing or inactivation of just one of these two genes induces the accumulation of Emi1 in prometaphase cells suggests that Emi1 is mostly targeted by β-Trcp1/β-Trcp2 heterodimers.

The results reported herein demonstrate a role for β-Trcp1 in the regulation of both meiosis and mitosis. In addition, these findings indicate that the mitotic ubiquitin ligase APC/C is controlled by an SCF ubiquitin ligase containing β-Trcp1 as the substrate-targeting subunit. Thus, SCF ligases act not only in interphase, as generally believed, but also regulate the timely progression through mitosis.

Experimental Procedures

Generation of β-Trcp1$^{-/-}$ Mice

A full-length human β-Trcp1 cDNA was used to screen a λFIX II mouse genomic library of 129SV/J strain (Stratagene). To confirm the identities of genomic clones, phage DNA was digested with XbaI and the genomic fragments were subcloned into pBSK and analyzed by Southern blot and DNA sequencing. A 5.2 Kbp NotI-XhoI genomic fragment containing two exons downstream of exon 5 (the F box-encoding exon) was subcloned into the NotI-XhoI site of the pPNT targeting vector (Tybulewicz et al., 1991). A 3.8 Kbp intron fragment extending from the XhoI site downstream of exon 4 to codon 153 within exon 5 was modified with XbaI linkers and subcloned into the XbaI site of pPNT between the *neo*^{R} and thymidine kinase genes. The resultant targeting vector has a large portion of exon 5 that encodes the almost complete F box of β-Trcp1 plus an additional 22 amino acid region downstream of the F box (in total amino acids 154–212) deleted. This placed the *neo*^{R} gene in an antisense orientation and stop codons in all three reading frames within exon 5 at amino acid 153. In addition, the splicing acceptor site of exon 5 was left intact. Finally, exons 6 and 7 are not in-frame with exon 4. This makes it unlikely to splice from exon 4 to exon 6 or 7, which would generate a truncated form of β-Trcp1 protein. The targeting vector was linearized and electroporated into D3 embryonic stem cells. Clones doubly resistant to G418 (300 μg/ml) and gancyclovir (2 μM) were tested for homologous recombination by Southern analysis. Two genomic probes were used to confirm that homologous recombination had occurred using HindIII or XbaI digests (in Figure 1A, HindIII sites are indicated as H and XbaI sites as X). A *neo*^{R} gene probe was used to insure that random integration of the targeting vector had not occurred elsewhere in the genome. Male chimeras produced F1 agouti animals, 50% of which were F1 heterozygotes. Male and female F1 heterozygotes identified by Southern or genomic PCR analysis were interbred to produce F2 progeny. A genomic PCR assay (Figure 1C) to detect the wild-type allele (372 bp) or the

MEFs were transfected with either Myc-tagged wild-type Emi1 (second panel from the top) or Myc-tagged Emi1(S145A/S149A) mutant (bottom panel). Twenty-four hours later, prometaphase cells were plated in the presence of cycloheximide. At the indicated times, MEFs were collected and lysed, and extracts were subjected to immunoblotting with antibodies to Myc (to detect exogenous Myc-tagged Emi1) and Cul1.

(C) Purified recombinant β-Trcp1 rescues the ability of an extract from β-Trcp1$^{-/-}$ MEFs to ubiquitinylate Emi1 in vitro. In vitro ubiquitin ligation of in vitro translated Emi1 was carried out with prometaphase extracts from wild-type MEFs (lanes 1–4) or β-Trcp1-deficient MEFs in the absence (lanes 5–8) or the presence (9–12) of purified recombinant SCF$^{β\text{-Trcp1}}$. The small bracket on the left side of the panels marks Emi1, which progressively upshifted with time, likely because of phosphorylation events. The larger bracket marks a ladder of bands >50,000 corresponding to polyubiquitinylated Emi1.

(D) β-Trcp1 binding to Emi1 depends on the DSGxxS motif present in Emi1. HeLa cells were transfected with an empty vector (lanes 1, 5, and 8), Flag-tagged β-Trcp1 (lanes 2, 6, 7, 9, and 10), Flag-tagged Fbw4 (lane 3), and Flag-tagged Fbw5 (lane 4) alone or in combination with either Myc-tagged Emi1 (lanes 5, 6, 8, and 9) or Emi1(S145A/S149A) mutant (lanes 7 and 10). Cells were treated overnight with nocodazole and with the proteasome inhibitor ZLLL for 3 hr prior to their harvesting and lysis. Extracts were either subjected to immunoprecipitation (IP) with an anti-Flag antibody followed by immunoblotting (IB) as indicated (lanes 1–7), or directly to immunoblotting to check levels of expression of wild-type and mutant Emi1 proteins (lanes 8–10).

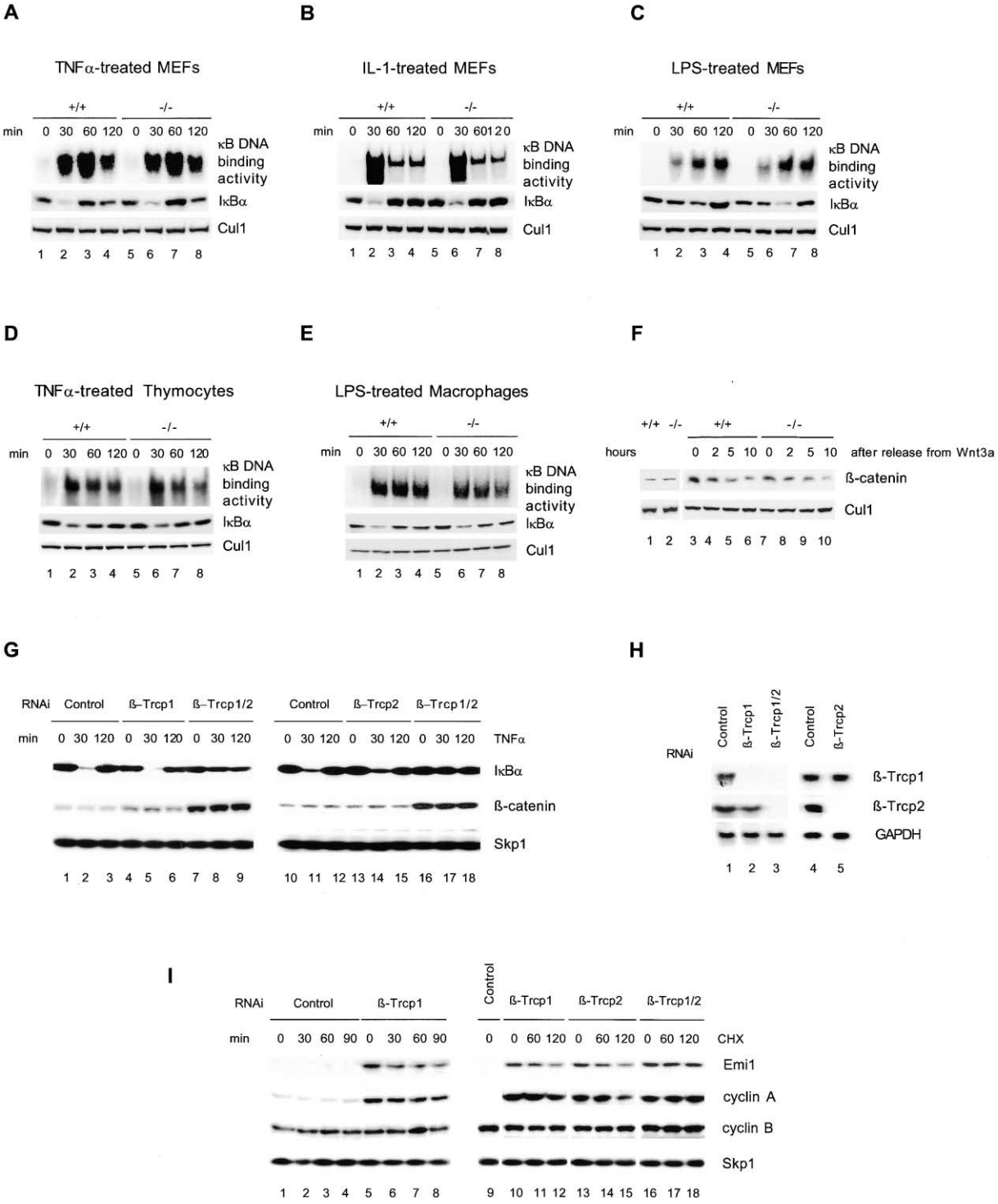

Figure 7. β-Trcp1 and β-Trcp2 Are Redundant in Controlling the Stability of IκBα and β-Catenin

(A–E) IκBα degradation and NFκB DNA binding activity are not affected by β-Trcp1 deficiency. NFκB activity was stimulated in MEFs (A–C), thymocytes (D), and macrophages (E) with the indicated stimuli. Cells were then collected at the indicated times and lysed. Extracts were subjected to electrophoretic mobility shift assay performed as described (Beg et al., 1993) using the palindromic κB probe (Bours et al., 1992; top panels) or to immunoblotting with antibodies to IκBα and Cul1.

(F) β-catenin degradation is not affected by β-Trcp1 deficiency. MEFs were treated with Wnt3a to induce β-catenin. Two hours after treatment (indicated as time 0), cells were washed and collected at the indicated times. Extracts were subjected to immunoblotting with antibodies to β-catenin and Cul1 (used as a loading control). Lanes 1 and 2 show basal levels of β-catenin (prior to Wnt3a treatment).

(G and H) Silencing of both β-Trcp1 and β-Trcp2 stabilizes IκBα and β-catenin.

(G) HeLa cells were transfected two times every 24 hr with siRNA molecules corresponding to a nonrelevant Fbp (lanes 1–3 and 10–12), β-Trcp1 (lanes 4–6), β-Trcp2 (lanes 13–15), or to both β-Trcp1 and β-Trcp2 (β-Trcp1/2; lanes 7–9 and 16–18). Forty-eight hours after the last

mutant β-Trcp1 allele (261 bp) was designed using a common D3 primer (5′-CTTCCTTATCTAACAGAAGATGGA-3′) and either the β-Trcp1 wild-type exon D1 primer (5′-TCCTGACCATCCTCTCGATG AGC-3′) or the *neo*^{R} gene L90 primer (5′-TCTAATTCCATCAGAAGCTG ACT-3′).

Autopsy and Histopathology

Approximately 35 mice for each genotype at 1 and 1.5 year time points and approximately 15 mice for each genotype between 6 and 9 months were autopsied and all tissues were examined for gross abnormality. Tissues were formalin fixed, dehydrated, and embedded in paraffin according to standard protocols. Sections (5 μm) were stained with hematoxylin and eosin (H&E) and examined microscopically. Testes were isolated and punctured for effective penetration of the fixative. Testes and epididymes were fixed for 48 hr in 10% PBS-buffered formalin at room temperature and embedded in paraffin. Mounted sections were deparaffinized, rehydrated, and stained with H&E or with periodic acid Schiff (PAS).

Cells, Cell Cycle Analyses, and Transient Transfections

Primary MEFs were obtained from 12.5-day-old embryos as described (Yamasaki et al., 1996). T cells and peritoneal macrophages were isolated according to published protocols (Latres et al., 2001; Jin and Conti, 2002). MEFs were synchronized in G0/G1 using low serum and in G1/S using aphidicolin as described (O'Connor and Jackman, 1995). MEFs and HeLa cells were synchronized in prometaphase with 6–12 hr nocodazole treatment followed by mitotic shake-off as described (Carrano et al., 1999). Cell cycle synchrony was monitored by flow cytometry and BrdU incorporation as described (Carrano and Pagano, 2001). Cells were transfected with FuGENE transfection reagent (Roche) according to the manufacturer's instructions.

Immunological Procedures

Rabbit polyclonal antibody (Pab) to β-Trcp1 was generated using the recombinant His-β-Trcp1 C-terminal fragment (residues 180–569), and Pab to Emi1 was against GST-Emi1. Rabbit Pabs to Cul1 (Latres et al., 1999), cyclin A (Carrano et al., 1999), cyclin B (Carrano and Pagano, 2001), and Emi1 (Hsu et al., 2002) were previously described. Mouse monoclonal antibodies to α-tubulin, Flag, and Myc were from Sigma, to β-catenin from BD-Transduction labs, to Skp1 from Zymed, and to BrdU from Roche. Rabbit Pabs to phosphorylated Histone H3 was from Upstate, to IκBα from Santa Cruz, and to γ-tubulin from Sigma. Unless specified, protein extraction was performed as described (Carrano et al., 1999). Immunoblot analysis and immunoprecipitations were performed as described (Carrano et al., 1999).

In Vivo Degradation Assays and In Vitro Ubiquitinylation Assay

Wnt3a-transfected L cells (Shibamoto et al., 1998) were used as a source of Wnt3a-conditioned medium. MEFs were Wnt3a stimulated for 2 hr, then released in fresh medium, collected, and extracted as described (Liu et al., 2002). IκBα degradation experiments were performed by incubating MEFs with TNFα (10 ng/ml), IL-1 (10 ng/ml), LPS (10 μg/ml), PMA (100 ng/ml), sorbitol (0.6 M), tunicamycin (100 μg/ml), and H_2O_2 (100 μM). At the indicated times, MEFs were collected and extracted according to Beg et al. (1993).

Two microliters of in vitro translated ^{35}S-labeled Emi1 were incubated at 30°C in 10 μl of ubiquitinylation mix (Montagnoli et al., 1999) containing 20 μg of cell extract obtained from prometaphase MEFs as described (Montagnoli et al., 1999). Where indicated, approximately 5 ng of purified recombinant SCF complexes were added. Reaction products were run on SDS-PAGE followed by autoradiography. Roc1/Ha-Cul1/His-Skp1/β-Trcp1 and Roc1/Ha-Cul1/His-Skp1/Skp2 complexes were expressed in 5B insect cells and purified by nickel-agarose chromatography as described (Carrano et al., 1999; Latres et al., 1999).

Immunofluorescence

Cells were plated on glass coverslips coated (overnight at 4°C) with poly-L-lysine (100 μg/ml in PBS), rinsed in PBS, and fixed for 10 min in 4% paraformaldehyde/PBS at room temperature. For centrosomal staining only, cells were fixed for 10 min in cold methanol (−20°C). Fixed cells were permeabilized with PBS/0.1% Triton X-100 for 3 min, washed in PBS, and blocked with PTB buffer (PBS/0.1% Triton X-100/0.3% BSA) for 30 min at room temperature. Incubation with primary antibodies was then carried out for 1–3 hr in a humidified chamber. After three washes in PBS, the coverslips were incubated for 30 min with Texas red-conjugated or FITC-conjugated secondary antibody. All antibody reactions were carried out at room temperature and dilutions were made in PTB buffer. Samples were mounted in crystal/mount medium containing DAPI to identify nuclei.

Silencing by Small Interfering RNA

Logarithmically growing HeLa cells were seeded at a density of 10^5 cells/6 cm dish and transfected with oligomers twice (at 24 and 48 hr after replating) using Oligofectamine (Invitrogen). Forty-eight hours after the last transfection, lysates were prepared and analyzed by SDS-PAGE and immunoblotting. The siRNA oligomers used for β-Trcp1 silencing were 21 bp synthetic molecules corresponding to nt 195–213 (oligo L, CCC AGG GAC UGG CGC ACU CdTdT) and nt 1082–1100 (oligo H, UUC UCA CAG GCC AUA CAG GdTdT) of the human β-Trcp1 coding region (NM_033637). For β-Trcp2 silencing, we used an oligomer corresponding to nt 183–203 (oligo D, GAG GCC AUC AGA AGG AAA CdTdT) of the human β-Trcp2 coding region (AB033279). We also used an siRNA oligomer corresponding to both nt 515–535 of human β-Trcp1 and nt 262–282 of human β-Trcp2 (oligo 1/2, GUG GAA UUU GUG GAA CAU CdTdT).

Acknowledgments

We thank R. Bronson, T. Bashir, L. Di Marcotullio, V. Dorrello, G. Draetta, and A. Peschiaroli for their contribution to this work; K. Nakayama for communicating his results prior to publication; J. Bloom, A. Hershko, K. Manova, and D. Wolgemuth for helpful discussions; A. Beg, Y. Ben-Neriah, A. Darwin, G. Franzoso, S. Fuchs, M. Philips, D. Levy, A. Pellicer, V. Spiegelman, and Y. Weinrauch for reagents and suggestions. M.P. is grateful to T.M. Thor for continuous support. This work was supported by an Italian American Cancer Foundation fellowship (1999-2000) and a Susan Komen Breast Cancer Foundation fellowship (2001 to present) to D.G., a fellowship from the Japanese Ministry of Education, Culture, Sports, Science, and Technology (2001) and the International Agency for Research on Cancer fellowship (2002) to Y.K., an Irma Hirschl Scholarship and grants from the NIH (R01-CA76584 and R01-GM57587) to M.P.; and a Pew Scholarship and an NIH grant (R01-CA79646) to L.Y.

Received: December 19, 2002
Revised: March 25, 2003
Accepted: April 3, 2003
Published: June 2, 2003

References

Bai, C., Sen, P., Hofman, K., Ma, L., Goebel, M., Harper, W., and Elledge, S. (1996). Skp1 connects cell cycle regulators to the ubiquitin proteolysis machinery through a novel motif, the F-box. Cell *86*, 263–274.

transfection, cells were treated with TNFα to stimulate IκBα degradation. At the indicated times, cells were harvested and cell extracts were analyzed by immunoblotting with antibodies to the indicated proteins.
(H) Aliquots at time 0 were used to analyze the expression of β-Trcp1 (top panel), β-Trcp2 (middle panel), and GAPDH (bottom panel) mRNAs.
(I) Silencing of either β-Trcp1 or β-Trcp2 induces stabilization of Emi1 in mitotic HeLa cells. Thirty-two hours after the last transfection with the indicated oligomers, nocodazole was added for an additional 16 hr. Prometaphase cells were plated in the presence of cycloheximide for the indicated times. Cells were then harvested and cell extracts were analyzed by immunoblotting with antibodies to the indicated proteins.

Beg, A., Finco, T., Nantermet, P., and Baldwin, A., Jr. (1993). Tumor necrosis factor and interleukin-1 lead to phosphorylation and loss of IκBα: a mechanism for NF-κB activation. Mol. Cell. Biol. *13*, 3301–3310.

Bours, V., Burd, P., Brown, K., Villalobos, J., Park, S., Ryseck, R., Bravo, R., Kelly, K., and Siebenlist, U. (1992). A novel mitogen-inducible gene product related to p50/p105-NF-κB participates in transactivation through a κB site. Mol. Cell. Biol. *12*, 685–695.

Carrano, A., and Pagano, M. (2001). Role of Skp2 in adhesion-dependent cell cycle progression. J. Cell Biol. *153*, 1381–1389.

Carrano, A., Eytan, E., Hershko, A., and Pagano, M. (1999). Skp2 is required for the ubiquitin-mediated degradation of the Cdk-inhibitor p27. Nat. Cell Biol. *1*, 193–199.

Cenciarelli, C., Chiaur, D., Guardavaccaro, D., Parks, W., Vidal, M., and Pagano, M. (1999). Identification of a human family of F-box proteins. Curr. Biol. *9*, 1177–1179.

Fuchs, S., Chen, A., Xiong, Y., Pan, Z.Q., and Ronai, Z. (1999). HOS, a human homolog of Slimb, forms an SCF complex with Skp1 and Cullin1 and targets the phosphorylation-dependent degradation of IκB and β-catenin. Oncogene *18*, 2039–2046.

Girard, F., Fernandez, A., and Lamb, S. (1995). Delayed cyclin A and B1 degradation in non-transformed mammalian cells. J. Cell Sci. *108*, 2599–2608.

Grosskortenhaus, R., and Sprenger, F. (2002). Rca1 inhibits APC-Cdh1(Fzr) and is required to prevent cyclin degradation in G2. Dev. Cell *2*, 29–40.

Hansen, D., Hsu, J., Kaiser, B., Jackson, P., and Eldridge, A. (2002). Control of the centriole and centrosome cycles by ubiquitination enzymes. Oncogene *21*, 6209–6221.

Hart, M., Concordet, J., Lassot, I., Albert, I., Durand, H., Perret, C., Rubinfeld, B., Margottin, F., Benarous, R., and Polakis, P. (1999). The F-box protein β-TrCP associates with phosphorylated β-catenin and regulates its activity in the cell. Curr. Biol. *9*, 207–210.

Hatakeyama, S., Kitagawa, M., Nakayama, K., Shirane, M., Matsumoto, M., Hattori, K., Higashi, H., Nakano, H., Okumura, K., Onoe, K., et al. (1999). Ubiquitin-dependent degradation of IκBα is mediated by a ubiquitin ligase Skp1/Cul1/F-box protein Fwd1. Proc. Natl. Acad. Sci. USA *96*, 3859–3863.

Hattori, K., Hatakeyama, S., Shirane, M., Matsumoto, M., and Nakayama, K. (1999). Molecular dissection of the interactions among IκBα, FWD1, and Skp1 required for ubiquitin-mediated proteolysis of IκBα. J. Biol. Chem. *274*, 29641–29647.

Hsu, J., Reimann, J., Sorensen, C., Lukas, J., and Jackson, P. (2002). E2F-dependent accumulation of hEmi1 regulates S phase entry by inhibiting APC(Cdh1). Nat. Cell Biol. *4*, 358–366.

Jin, S., and Conti, M. (2002). Induction of the cyclic nucleotide phosphodiesterase PDE4B is essential for LPS-activated TNF-α responses. Proc. Natl. Acad. Sci. USA *99*, 7628–7633.

Kipreos, E., and Pagano, M. (2000). The F-box protein family. Genome Biol. *1*, 3001–3007.

Kitagawa, M., Hatakeyama, S., Shirane, M., Matsumoto, M., Ishida, N., Hattori, K., Nakamichi, I., Nakayama, K., and Nakayama, K. (1999). An F-box protein, FWD1, mediates ubiquitin-dependent proteolysis of β-catenin. EMBO J. *18*, 2401–2410.

Koike, J., Sagara, N., Kirikoshi, H., Takagi, A., Miwa, T., Hirai, M., and Katoh, M. (2000). Molecular cloning and genomic structure of the β-TRCP2 gene on chromosome 5q35.1. Biochem. Biophys. Res. Commun. *269*, 103–109.

Kroll, M., Margottin, F., Kohl, A., Renard, P., Durand, H., Concordet, J., Bachelerie, F., Arenzana, F., and Benarous, R. (1999). Inducible degradation of IκBα by the proteasome requires interaction with the F-box protein β-TrCP. J. Biol. Chem. *274*, 7941–7945.

Latres, E., Chiaur, D., and Pagano, M. (1999). The human F-box protein β-Trcp associates with the Cul1/Skp1 complex and regulates the stability of β-catenin. Oncogene *18*, 849–855.

Latres, E., Chiarle, R., Schulman, B., Pellicer, A., Inghirani, G., and Pagano, M. (2001). Role of the F-box protein Skp2 in lymphomagenesis. Proc. Natl. Acad. Sci. USA *98*, 2515–2520.

Liu, C., Li, Y., Semenov, M., Han, C., Baeg, G., Tan, Y., Zhang, Z., Lin, X., and He, X. (2002). Control of β-catenin phosphorylation/degradation by a dual-kinase mechanism. Cell *108*, 837–847.

Maruyama, S., Hatakeyama, S., Nakayama, K., Ishida, N., and Kawakami, K. (2001). Characterization of a mouse gene (*Fbxw6*) that encodes a homologue of *Caenorhabditis elegans SEL-10*. Genomics *78*, 214–222.

Montagnoli, A., Fiore, F., Eytan, E., Carrano, A., Draetta, G., Hershko, A., and Pagano, M. (1999). Ubiquitination of p27 is regulated by Cdk-dependent phosphorylation and trimeric complex formation. Genes Dev. *13*, 1181–1189.

O'Connor, P., and Jackman, J. (1995). Synchronization of mammalian cells. In Cell Cycle: Materials and Methods, M. Pagano, ed. (New York: Springer-Verlag), pp. 63–74.

Peters, J.M. (2002). The anaphase-promoting complex: proteolysis in mitosis and beyond. Mol. Cell *9*, 931–943.

Piva, R., Liu, J., Chiarle, R., Podda, A., Pagano, M., and Inghirani, G. (2002). In vivo interference with Skp1 function leads to genetic instability and neoplastic transformation. Mol. Cell. Biol. *22*, 8375–8387.

Reimann, J., and Jackson, P. (2002). Emi1 is required for cytostatic factor arrest in vertebrate eggs. Nature *416*, 850–854.

Reimann, J., Freed, E., Hsu, J., Kramer, E., Peters, J.M., and Jackson, P. (2001). Emi1 is a mitotic regulator that interacts with Cdc20 and inhibits the anaphase promoting complex. Cell *105*, 645–655.

Shibamoto, S., Higano, K., Takada, R., Ito, F., Takeichi, M., and Takada, S. (1998). Cytoskeletal reorganization by soluble Wnt-3a protein signalling. Genes Cells *3*, 659–670.

Shirane, M., Hatakeyama, S., Hattori, K., and Nakayama, K. (1999). Common pathway for the ubiquitination of IκBα, IκBβ, and IκBε mediated by the F-box protein FWD1. J. Biol. Chem. *274*, 28169–28174.

Spencer, E., Jiang, J., and Chen, Z.J. (1999). Signal-induced ubiquitination of IκB by the F-box protein Slimb/β-TrCP. Genes Dev. *13*, 284–294.

Suzuki, H., Chiba, T., Kobayashi, M., Takeuchi, M., Suzuki, T., Ikenoue, T., Omata, M., Furuichi, K., and Tanaka, K. (1999). IκBα ubiquitination is catalyzed by an SCF complex containing Skp1, Cul1, and two F-box/WD40-repeat proteins, β-TrCP1 and β-TrCP2. Biochem. Biophys. Res. Commun. *256*, 127–132.

Suzuki, H., Chiba, T., Suzuki, T., Fujita, T., Ikenoue, T., Omata, M., Furuichi, K., Shikama, H., and Tanaka, K. (2000). Homodimer of two F-box proteins β -Trcp1 or β -Trcp2 binds to IκBα for signal-dependent ubiquitination. J. Biol. Chem. *275*, 2877–2884.

Tan, P., Fuchs, S., Chen, A., Wu, K., Gomez, C., Ronai, S., and Pan, Z. (1999). Recruitment of a ROC1-CUL1 ubiquitin ligase by Skp1 and HOS to catalyze the ubiquitination of IκBα. Mol. Cell *3*, 527–533.

Tybulewicz, V., Crawford, C., Jackson, P., Bronson, R., and Mulligan, R.C. (1991). Neonatal lethality and lymphopenia in mice with a homozygous disruption of the c-abl proto-oncogene. Cell *65*, 1153–1163.

Winston, J., Strack, P., Beer, P., Chu, C., Elledge, S., and Harper, W. (1999). The $SCF^{\beta\text{-}TRCP}$ ubiquitin ligase complex associates specifically with phosphorylated destruction motifs in IκBα and β-catenin and stimulates IκBα ubiquitination in vitro. Genes Dev. *13*, 270–283.

Wojcik, E., Glover, D., and Hays, T. (2000). The SCF ubiquitin ligase protein slimb regulates centrosome duplication in *Drosophila*. Curr. Biol. *10*, 1131–1134.

Wu, C., and Ghosh, S. (1999). β-TrCP mediates the signal-induced ubiquitination of IκBβ. J. Biol. Chem. *274*, 29591–29594.

Yamasaki, L., Jacks, T., Bronson, R., Goillot, E., Harlow, E., and Dyson, N. (1996). Tumor induction and tissue atrophy in mice lacking E2F-1. Cell *85*, 537–548.

Yaron, A., Hatzubai, A., Davis, M., Lavon, I., Amit, S., Manning, A., Andersen, J., Mann, M., Mercurio, F., and Ben, N.Y. (1998). Identification of the receptor component of the IκBα-ubiquitin ligase. Nature *396*, 590–594.